Molecular Biology of the Cell
Vol. 19, 3290–3298, August 2008

Atg8 Controls Phagophore Expansion during Autophagosome Formation

Zhiping Xie,* Usha Nair,* and Daniel J. Klionsky*†

*Life Sciences Institute and Department of Molecular, Cellular, and Developmental Biology, and †Department of Biological Chemistry, University of Michigan, Ann Arbor, MI 48109

Submitted January 2, 2008; Revised April 21, 2008; Accepted May 16, 2008
Monitoring Editor: Howard Riezman

Autophagy is a potent intracellular degradation process with pivotal roles in health and disease. Atg8, a lipid-conjugated ubiquitin-like protein, is required for the formation of autophagosomes, double-membrane vesicles responsible for the delivery of cytoplasmic material to lysosomes. How and when Atg8 functions in this process, however, is not clear. Here we show that Atg8 controls the expansion of the autophagosome precursor, the phagophore, and give the first real-time, observation-based temporal dissection of the autophagosome formation process. We demonstrate that the amount of Atg8 determines the size of autophagosomes. During autophagosome biogenesis, Atg8 forms an expanding structure and later dissociates from the site of vesicle formation. On the basis of the dynamics of Atg8, we present a multistage model of autophagosome formation. This model provides a foundation for future analyses of the functions and dynamics of known autophagy-related proteins and for screening new genes.

INTRODUCTION

Eukaryotic cells employ macroautophagy, hereafter referred to as autophagy, to eliminate objects ranging from soluble proteins to entire organelles (Yorimitsu and Klionsky, 2005; Xie and Klionsky, 2007). In multicellular organisms, autophagy has important roles in development, immune defense, programmed cell death, tumor suppression, and the prevention of neuronal degeneration (Levine and Klionsky, 2004; Shintani and Klionsky, 2004a; Boland and Nixon, 2006; Schmid and Münz, 2007). In this pathway, cytoplasmic materials are sequestered into an expanding membrane sac, the phagophore, which subsequently matures into a double-membrane vesicle, the autophagosome. The site of autophagosome formation is termed the phagophore assembly site (PAS; Kim *et al.*, 2002; Suzuki *et al.*, 2001). Each autophagosome eventually fuses with a lysosome, resulting in the degradation of the inner membrane and the cargos. The formation of autophagosomes depends on the concerted actions of core autophagy machinery proteins (Yorimitsu and Klionsky, 2005; Xie and Klionsky, 2007).

Among the core machinery proteins is Atg8, a ubiquitin-like protein (Ichimura *et al.*, 2000; Paz *et al.*, 2000). Newly synthesized Atg8 is processed by a cysteine protease, Atg4, to expose its carboxyl terminal glycine residue (Kirisako *et al.*, 2000; Kim *et al.*, 2001; Hemelaar *et al.*, 2003). It is then conjugated to phosphatidylethanolamine (PE) by the E1-like activating enzyme Atg7 and the E2-like conjugating enzyme Atg3 (Tanida *et al.*, 1999; Ichimura *et al.*, 2000; Tanida *et al.*, 2001, 2002). Conjugated Atg8 can also be deconjugated by Atg4 (Kirisako *et al.*, 2000). A multimeric protein complex formed by Atg12, Atg5, and Atg16 facilitates the conjugation of Atg8, possibly by serving as an E3-like enzyme (Suzuki *et al.*, 2001; Hanada *et al.*, 2007). The formation of this complex itself also involves a conjugation reaction, in which the ubiquitin-like protein Atg12 is attached to Atg5 by Atg7 and the E2-like enzyme Atg10 (Mizushima *et al.*, 1998a,b, 2003; Kuma *et al.*, 2002).

During autophagy, Atg8 localizes to the PAS. In addition to PE conjugation and the Atg12–Atg5-Atg16 complex, its proper localization requires Atg9, a transmembrane protein suggested as a membrane carrier, and the autophagy-specific phosphatidylinositol 3-kinase (PI3K) complex (Kametaka *et al.*, 1998; Kirisako *et al.*, 2000; Kim *et al.*, 2001; Suzuki *et al.*, 2001, 2007; Reggiori *et al.*, 2005; Young *et al.*, 2006). The PAS population of Atg8 is presumably associated with the phagophore (Kirisako *et al.*, 1999; Kabeya *et al.*, 2000, 2004). When the phagophore matures into an autophagosome, some Atg8 is trapped inside and eventually degraded (Kirisako *et al.*, 1999; Huang *et al.*, 2000; Kabeya *et al.*, 2000; Tanida *et al.*, 2005). The absence of Atg8 does not apparently affect the function of any other core machinery proteins (Suzuki *et al.*, 2001, 2007). Although Atg8 has been widely used as a marker for recognition of autophagosomes (Klionsky *et al.*, 2007), its exact in vivo function is still not clear.

In the yeast *Saccharomyces cerevisiae*, the core machinery proteins are shared between starvation-induced autophagy and a second autophagy-like process, the cytoplasm to vacuole targeting (Cvt) pathway, which transports hydrolase precursors from the cytosol to the vacuole (a lysosome analogue) under nutrient-rich conditions (Baba *et al.*, 1997; Xie and Klionsky, 2007). Among these proteins, only Atg8 has a significantly elevated protein level when autophagy is induced by starvation, making it a natural candidate for an autophagy regulator (Kirisako *et al.*, 1999; Huang *et al.*, 2000). Here we investigated the role of Atg8 through morphological and functional analyses.

This article was published online ahead of print in *MBC in Press* (http://www.molbiolcell.org/cgi/doi/10.1091/mbc.E07–12–1292) on May 28, 2008.

Address correspondence to: Daniel J. Klionsky (klionsky@umich.edu).

Abbreviations used: ALP, alkaline phosphatase; Atg, autophagy-related; Cvt, cytoplasm to vacuole targeting; GFP, green fluorescent protein; prApe1, precursor aminopeptidase I.

MATERIALS AND METHODS

Yeast Media

The media used were as follows: rich medium (YPD): 1% yeast extract, 2% peptone, and 2% glucose; and nitrogen starvation medium (SD-N): 2% glucose, and 0.17% yeast nitrogen base without amino acids and ammonium sulfate.

Construction of Strains and Plasmids

Gene knockouts were performed as previously described (Yen *et al.*, 2007). To construct Atg8 expression plasmids, promoters from genes with protein levels expected to be similar to that of Atg8 in rich medium were placed in front of the *ATG8* open reading frame; the resulting Atg8 protein levels were tested by Western blotting. Three plasmids were chosen for this study based on the following two criteria: 1) Atg8 amounts in starvation were lower than that of the wild-type strain and 2) Atg8 amounts in rich media were similar to that of the wild-type strain. Plasmid $pP_{ATG27}ATG8(406)$ contains 740 base pairs of *ATG27* 5′ sequence; plasmid $pP_{VPS30}ATG8\text{-}P_{ATG18}ATG8(406)$ contains 420 base pairs of *VPS30* 5′ sequence and 530 base pairs of *ATG18* 5′ sequence in front of two copies of *ATG8* open reading frames, respectively; plasmid $pP_{ATG3}ATG8(406)$ contains 380 base pairs of *ATG3* 5′ sequence. Plasmid pP_{1K}*Green fluorescent protein (GFP)-ATG8(406)* contains 990 base pairs of *ATG8* 5′ sequence in front of the GFP-Atg8 open reading frame. These Atg8-expressing plasmids or the corresponding empty vectors were linearized and integrated into the *atg8*Δ strain. The strains used in this study are listed in Table 1.

Electron Microscopy

Sample preparation and image acquisition were performed as described previously (Yen *et al.*, 2007). Autophagic body cross-sections with a clear limiting membrane were outlined by hand using Adobe Photoshop (San Jose, CA). The area values of outlined autophagic body cross-sections were obtained using the particle analysis function of ImageJ (http://rsb.info.nih.gov/ij/). The area values were then converted to radii for data presentation, using the formula: radius = square root of (area divided by pi).

Fluorescence Microscopy

Live cell fluorescence microscopy was performed as previously described (Yen *et al.*, 2007) with the following modification: one side of the cover glass was coated with 1 mg/ml concanavalin A for 5 min and rinsed with water; 100 μl of yeast cell culture was placed on the treated side for 3 min to immobilize yeast cells on the cover glass; the cover glass was rinsed with water, placed on a concavity slide containing liquid medium, and observed under the microscope.

Quantification of Fluorescence Intensity

At each time point, a stack of images was collected along the *z*-axis to cover the entire cell. A projection of the image stack was created by calculating the sum of signal intensities. The intensity of GFP-Atg8 puncta was calculated as the difference between the absolute value of the GFP-Atg8 punctum and that of the local background, using the intensity of its adjacent area, as determined with softWoRx software (Applied Precision, Issaquah, WA).

Additional Assays

The protein extraction, immunoblot and alkaline phosphatase (Pho8Δ60) assays were performed as described previously (Noda *et al.*, 1995; Yen *et al.*, 2007).

RESULTS

Atg8 Regulates the Level of Autophagy

To explore the possible role of Atg8 in autophagy regulation, we generated strains (A8-1, A8-2, and A8-3) that express different levels of Atg8 (Figure 1A; *Materials and Methods*). Under nitrogen-starvation conditions, the amounts of both conjugated and unconjugated Atg8 in these strains were lower than those of the wild type (Figure 1A). We then quantified the levels of autophagy in these strains using the Pho8Δ60 assay (Noda *et al.*, 1995). This assay is based on the autophagy-dependent delivery of a nonspecific cytosolic marker, the modified phosphatase precursor Pho8Δ60, from the cytosol to the vacuole, where it gets activated. The resulting alkaline phosphatase (ALP) activity thus indicates the total internal volume of the autophagosome population. In wild-type cells, nitrogen starvation led to a sharp increase of Pho8Δ60-dependent ALP activity (Figure 1B). In contrast, the *atg8*Δ strain showed a negligible increase. Strains A8-1, A8-2, and A8-3 showed intermediate increases, which correlated with their Atg8 protein levels. Importantly, these results were not caused by long-term low-level expression of Atg8 (i.e., a chronic defect), because in nutrient-rich media the levels of Atg8 in strains A8-1, A8-2, and A8-3 were similar to that of the wild-type strain (Figure 1A). This level of Atg8 was sufficient for the maturation of the Cvt pathway cargo, precursor aminopeptidase I (prApe1; Figure 1C). Thus, the levels of Atg8 directly determine levels of autophagy in the corresponding strains.

Atg8 Controls the Size of the Autophagosome

Normal recruitment of Atg8 to the PAS requires Atg9 (Suzuki *et al.*, 2001, 2007). It has been shown that slowing the anterograde trafficking of Atg9 leads to retarded autopha-

Table 1. Yeast strains used in this study

Descriptive name	Strain name	Genotype	Reference
Pho8Δ60 parent	TN124	MATα *leu2-3,112 trp1 ura3-52 pho8::pho8Δ60 pho13::LEU2*	Noda *et al.* (1995)
	YZX200	TN124 *atg8Δ::KAN*	This study
*atg8*Δ	YZX231	TN124 *atg8Δ::KAN URA3 TRP1*	This study
Wild type	YXZ232	TN124 *URA3 TRP1*	This study
A8-1	YZX233	TN124 *atg8Δ::KAN* $pP^{a}{}_{ATG27}ATG8::URA3\ TRP1$	This study
A8-2	YZX234	TN124 *atg8Δ::KAN* $pP_{VPS30}ATG8\text{-}P_{ATG18}ATG8::URA3\ TRP1$	This study
A8-3	YZX235	TN124 *atg8Δ::KAN* $pP_{ATG3}ATG8::URA3\ TRP1$	This study
Wild type *pep4*Δ	YZX213	TN124 *URA3 pep4Δ::TRP1*	This study
*atg8*Δ *pep4*Δ	YZX214	TN124 *atg8Δ::KAN URA3 pep4Δ::TRP1*	This study
A8-1 *pep4*Δ	YZX216	TN124 *atg8Δ::KAN* $pP_{ATG27}ATG8::URA3\ pep4\Delta::TRP1$	This study
A8-2 *pep4*Δ	YZX211	TN124 *atg8Δ::KAN* $pP_{VPS30}ATG8\text{-}P_{ATG18}ATG8::URA3\ pep4\Delta::TRP1$	This study
A8-3 *pep4*Δ	YZX212	TN124 *atg8Δ::KAN* $pP_{ATG3}ATG8::URA3\ pep4\Delta::TRP1$	This study
GA8	YZX247	TN124 *atg8Δ::KAN* $pP_{1K}GFP\text{-}ATG8::URA3\ TRP1$	This study
GFP-Atg8 mCherry-prApe1	YZX261	TN124 *atg8Δ::KAN* $pP_{1K}GFP\text{-}ATG8::URA3\ mCherry\text{-}Ape1::TRP1$	This study
A81-GA8	YZX233	TN124 *atg8Δ::KAN* $pP_{ATG27}GFP\text{-}ATG8::URA3\ TRP1$	This study
GA8+A8	YZX268	TN124 *atg8Δ::KAN* $pP_{1K}GFP\text{-}ATG8::URA3\ pP_{ATG3}ATG8::TRP1$	This study
*atg1*Δ *pep4*Δ *vps4*Δ	JHY28	SEY6210 *atg1Δ::HIS5 S.p. pep4Δ::LEU2 vps4Δ::TRP1*	Yen *et al.* (2007)

[a] P, promoter.

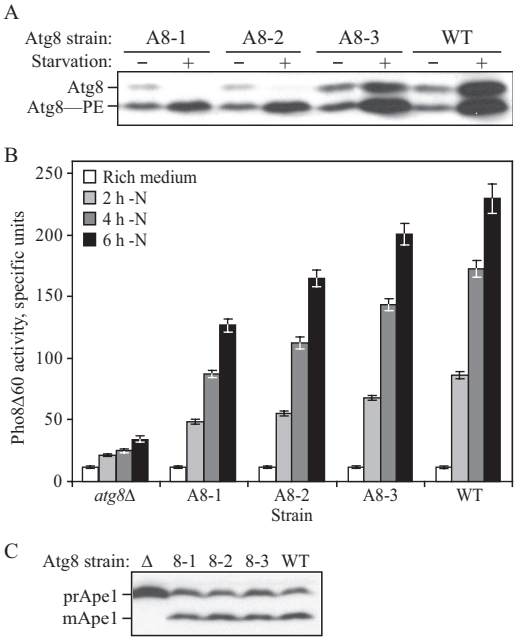

Figure 1. Atg8 regulates the level of autophagy. (A) Strains A8-1, A8-2, and A8-3 showed intermediate Atg8 protein levels. Yeast cells were grown in rich medium to midlog phase and then starved in nitrogen-starvation medium for 4 h. Protein extracts were analyzed by immunoblotting with anti-Atg8 antiserum. Atg8–PE, Atg8 conjugated to PE. (B) Atg8 limits the level of autophagy. Yeast cells were grown in rich medium to midlog phase and then shifted to nitrogen-starvation medium. At the indicated time points, samples were collected and tested by the Pho8Δ60 assay. Specific units, specific activity units (μmoles phosphate/mg/min) normalized to protein concentration. Error bar, SEM from six independent repeats. (C) The Cvt pathway is normal in strains A8-1, A8-2, and A8-3. Yeast cells grown in rich medium were collected at midlog phase; protein extracts were analyzed by immunoblotting with anti-Ape1 antiserum. The locations of precursor and mature Ape1 are indicated.

gosome formation without affecting autophagosome size, possibly by reducing the membrane supply (Yen *et al.*, 2007). To explore whether Atg8 functions in a similar manner, we analyzed the effect of lower Atg8 expression by transmission electron microscopy (EM).

Strains expressing variable levels of Atg8 were deleted for the *PEP4* locus. Pep4-dependent vacuolar hydrolase activity is required for degradation of the inner vesicles of autophagosomes (termed autophagic bodies) in the vacuole. Hence, the absence of *PEP4* allows the preservation of autophagic bodies. After 4 h of starvation, no autophagic bodies were observed in *atg8*Δ *pep4*Δ strains (Figure 2A), showing that *atg8*Δ cells are unable to produce autophagosomes; in A8-1, A8-2, A8-3, and wild-type strains deleted for *PEP4*, autophagic bodies abounded in the vacuoles (Figure 2A). Lower levels of Atg8 led to significant reductions in sizes of autophagosomes. The average cross-sectional radii of autophagic bodies in the A8-1, A8-2, and A8-3 *pep4*Δ strains were 115 ± 2, 125 ± 2, and 148 ± 2 nm, respectively, whereas that of the wild-type *pep4*Δ strain was 162 ± 2 nm (mean ± SEM, n > 200; Figure 2B). In contrast, the numbers of autophagic bodies were not affected by the reduced level of Atg8 at either 2 or 4 h of starvation (Figure 2C). These data suggest that even though Atg8 depends on Atg9 for its PAS localization, the role of Atg8 in autophagosome formation is distinct from that of Atg9, in that it specifically controls the size of autophagosomes.

The Dynamics of GFP-Atg8 during Autophagosome Formation

To gain further insight into how Atg8 participates in autophagosome formation, we used fluorescence microscopy to observe the dynamics of Atg8 in live cells. GFP-Atg8 was expressed under the control of the endogenous *ATG8* promoter in the *atg8*Δ background (strain GA8). When cells were examined under starvation conditions, we saw the constant emergence and disappearance of GFP-Atg8 punctate structures, each with a duration of ~10 min (Supplementary Movie S1, Supplementary Figure S1). The sizes of the GFP-Atg8 puncta expanded initially but then remained nearly the same when the fluorescence decreased (Supplementary Figure S2).

To determine whether this dynamic pattern correlates with autophagosome formation, we repeated the analysis in cells expressing mCherry-prApe1 (Figure 3A; Shaner *et al.*, 2004). Precursor Ape1 forms a large oligomer in the cytosol, detectable as a single punctum, which becomes a cargo of an autophagosome in starvation conditions (Baba *et al.*, 1997; Shintani *et al.*, 2002). Upon vacuolar delivery, the large oligomer disassembles into dodecamers, which then display a diffuse fluorescence pattern within the vacuole lumen. In wild-type cells, the disappearance of each mCherry-prApe1 punctum was preceded by the emergence and disappearance of a colocalizing GFP-Atg8 punctum. In contrast, in *atg1*Δ cells, which are defective in autophagosome formation (Tsukada and Ohsumi, 1993), both GFP-Atg8 and mCherry-prApe1 persisted without a significant decrease in fluorescence in punctate structures (Figure 3B). These data suggest that the dynamic pattern of Atg8 puncta formation and disassembly is an integral part of normal autophagy and that it represents events that occur before the disassembly of the cargo complex in the vacuole.

The Majority of Atg8 at the PAS Is Released during Autophagosome Formation

To test if the decrease and disappearance of the GFP-Atg8 signal represents the degradation of GFP-Atg8–containing autophagic bodies in the vacuole, we examined the dynamics of GFP-Atg8 in *pep4*Δ *atg11*Δ cells (*ATG11* was knocked out to reduce the accumulation of Cvt bodies, (Shintani and Klionsky, 2004b), which otherwise interfere in tracing the movement GFP-Atg8 puncta that are associated with autophagic bodies). A decrease of the GFP-Atg8 signal was again clearly observed (Figure 4A). After the decrease in GFP-Atg8 fluorescence, some GFP-Atg8 puncta persisted within the vacuole lumen, displaying a low amount of fluorescence, whereas the majority could no longer be detected. These data suggest that the majority of GFP-Atg8 molecules were released into the cytoplasm before autophagosome–vacuole fusion.

It should be noted that this large decrease of fluorescence was not an artifact due to photobleaching. We quantified the fluorescence of GFP-Atg8 puncta in live cells and compared them against the values obtained from fixed cells. In fixed cells, photobleaching caused less than a 10% reduction in fluorescence after 5 min (Figure 4, B and C). In contrast, in live *pep4*Δ *atg11*Δ cells and in GA8 cells, the fluorescence of GFP-Atg8 structures dropped well below 50% of the maximum intensities 5 min after the peak (Figure 4, B and C).

Next, we decided to test if the release of GFP-Atg8 fluorescence from the PAS required deconjugation. The deconjugation of Atg8–PE by Atg4 is necessary for normal autophagy (Kirisako *et al.*, 2000), although its exact role is not clear. We expressed GFP-Atg8ΔR, which lacks the carboxyl

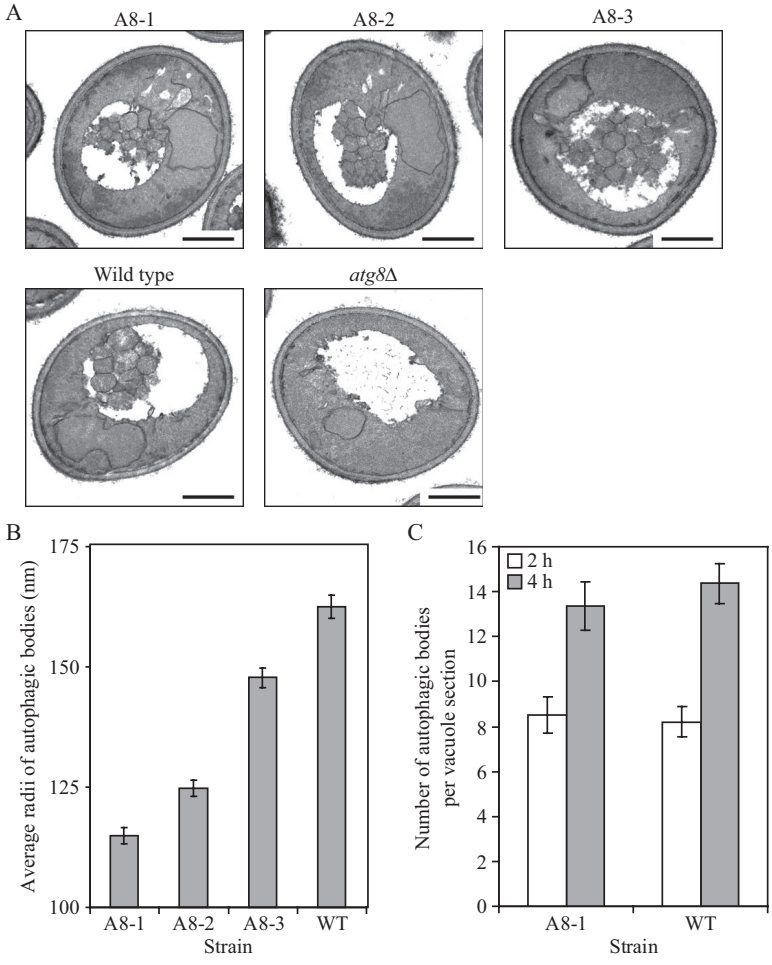

Figure 2. Atg8 controls the size of the autophagosome. (A and B) Lower amounts of Atg8 reduce the sizes of autophagosomes. Yeast cells were grown in rich medium to midlog phase and then starved in nitrogen-starvation medium for 4 h, fixed in potassium permanganate, and processed for EM. (A) Representative EM images from *pep4*Δ strains. Autophagic bodies accumulated in A8-1, A8-2, A8-3, and wild-type background strains. No autophagic bodies were found in *atg8*Δ background cells. Scale bar, 1 μm. (B) Quantification of autophagic body size. The average radii of cross-sections of autophagic bodies are shown; Error bar, SEM; n > 200. Autophagic bodies in the A8-1, A8-2, and A8-3 strains were significantly smaller than those of the wild-type (WT) background. (C) Atg8 level does not limit the number of autophagosomes produced. Yeast cells starved for 2 and 4 h were collected and processed for EM. The average numbers of autophagic bodies per vacuole section are shown. Error bar, SEM; n > 100. Similar numbers of autophagic bodies were observed in strains with different amounts of Atg8.

terminal arginine residue (thus bypassing the first step of Atg4 processing), together with mCherry-prApe1 in *atg4*Δ *atg8*Δ cells. In the absence of Atg4, Atg8ΔR can be conjugated normally but cannot be deconjugated. We then examined these cells in starvation conditions. As in wild-type cells, we found GFP-Atg8 puncta colocalizing with mCherry-prApe1, indicating that deconjugation is not required for the PAS localization of Atg8 (Figure 4D). However, these puncta did not show a significant decrease in fluorescence, and the colocalizing mCherry-prApe1 remained visible (Figure 4D), suggesting that the release of GFP-Atg8 from the PAS that we are monitoring is mediated by Atg4 and that this reaction is a crucial step in autophagosome formation and/or completion.

Taken together, these results suggest that each cycle of appearance and disappearance of the GFP-Atg8 signal represents the recruitment and release of Atg8 involved in the formation and completion of an autophagosome.

The Amount of the Atg8 at the PAS Regulates the Level of Autophagy

The PAS is generally considered to be the site where the core machinery proteins, including Atg8, act to form autophagosomes. We next tested whether the regulation of the level of autophagy that occurs through modulating the size of the autophagosome is accomplished by controlling the amount of Atg8 at the PAS. GFP-Atg8 was expressed in *atg8*Δ cells under the control of either its own promoter (strain GA8) or the promoter used in strain A8-1 (strain A81-GA8; Figure 5A). After cells were incubated in starvation conditions for 1 h, we quantified the peak fluorescence of the GFP-Atg8 PAS puncta during the dynamic cycles. The average intensity value in strain A81-GA8 was ~50% of that in strain GA8 (Figure 5B). Consistent with this observation, the Pho8Δ60 activity of strain A81-GA8 was lower than that of strain GA8 (Figure 5C), indicating that the amount of Atg8 recruited to the PAS regulates the level of autophagy.

Atg8 Does Not Control the Frequency of Autophagosome Formation

Our microscopy observation provided a novel method to test whether a lower amount of Atg8 limits the number of autophagosomes produced. Because the recruitment and release of the majority of Atg8 happens before the delivery of autophagosomes to the vacuole, the number of GFP-Atg8 signal peaks would reflect the number of autophagosomes formed. We compared the peak frequency in a strain (GA8) expressing GFP-Atg8 alone with that in a strain (GA8+A8) expressing additional Atg8 (Figure 6A). In strain GA8, the average number of peaks per cell in 15 min was 2.2 ± 0.1 (mean ± SEM). Strain GA8+A8 did not show a statistically significant difference in the frequency from strain GA8 (Figure 6B), even though the Pho8Δ60-dependent ALP activity was clearly higher in the former (Figure 6C), reflecting an increase in the total volume of the autophagosomes. This is consistent with our EM data, indicating

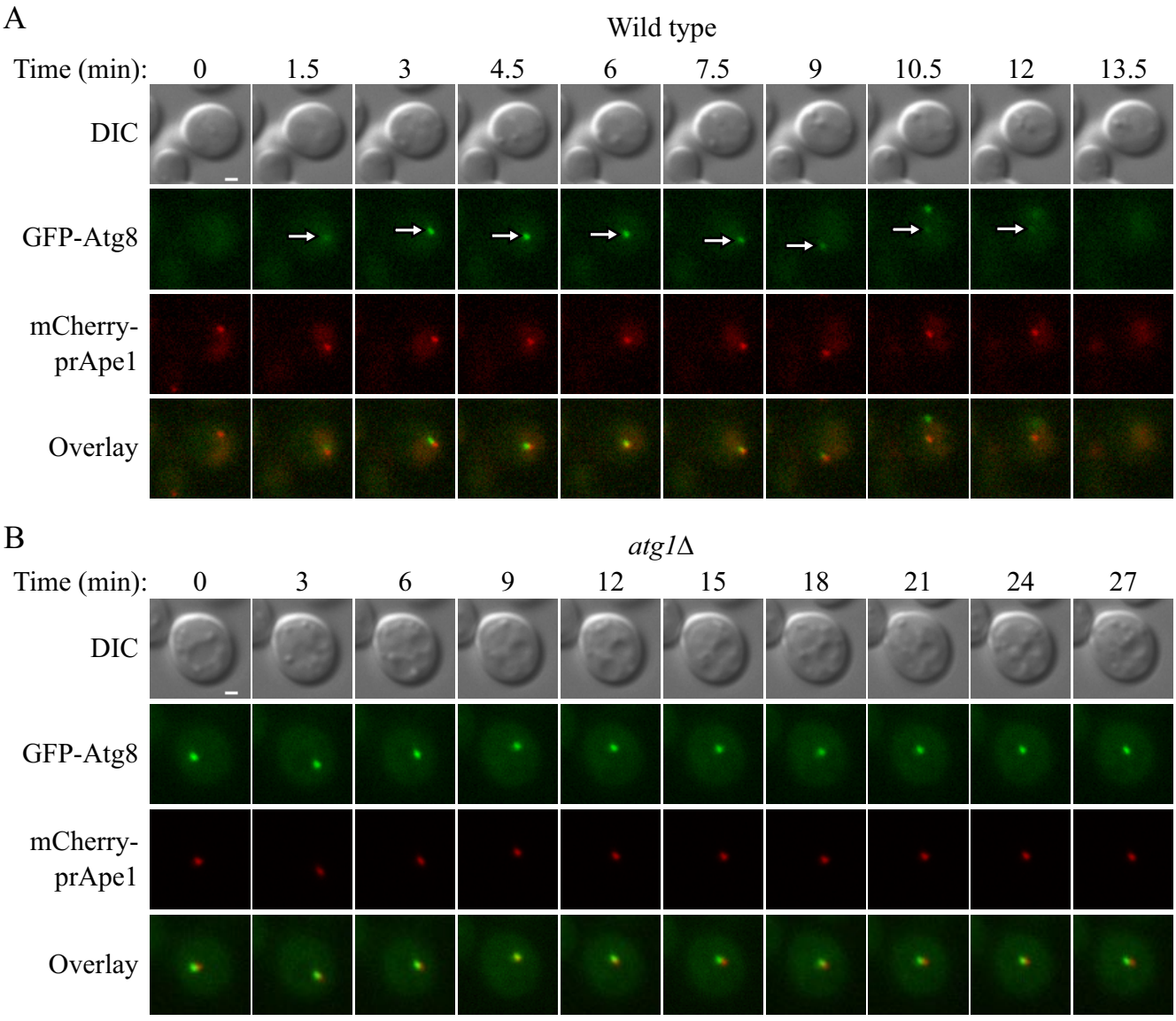

Figure 3. Dynamics of GFP-Atg8 during autophagosome formation. Yeast cells were grown in rich medium to midlog phase, then starved for 1 h, immobilized on concanavalin A-treated cover slips, and incubated in starvation medium on a depression (concave) slide. Image stacks were collected at the indicated time points; only the images with GFP-Atg8 puncta (if present) in focus are shown. (A) The emergence and disappearance of GFP-Atg8 puncta correspond to autophagosome formation. GFP-Atg8 and mCherry-prApe1 were expressed under their endogenous promoters in wild-type cells. GFP-Atg8 was recruited to the PAS, marked by the presence of the cargo mCherry-prApe1; after some GFP-Atg8 was released, the cargo was delivered to the vacuole and disassembled. The white arrow indicates the GFP-Atg8 punctum being tracked. (B) The dynamic pattern is absent in *atg1*Δ cells. GFP-Atg8 and mCherry-prApe1 were expressed in *atg1*Δ cells. GFP-Atg8 and mCherry-prApe1 signals persisted without a significant decrease in fluorescence in their punctate structures during 30 min of observation. DIC, differential interference contrast. Scale bar, 1 μm.

that a lower amount of Atg8 did not limit the rate of autophagosome formation but did affect autophagosome volume. In contrast, the frequency was significantly lower in *atg27*Δ cells (Figure 6B), which are known to produce fewer autophagosomes and served as a control (Yen *et al.*, 2007).

DISCUSSION

In this study, we showed that 1) the amount of Atg8 regulates the level of autophagy by specifically modulating the size of the autophagosomes, whereas the number of autophagosomes is unaffected, 2) each round of autophagosome formation involves a cycle of Atg8 trafficking in which Atg8 is first recruited to an expanding structure and later released from it, and 3) the release of Atg8 is essential for the completion of autophagosome formation and is mediated by deconjugation. In mammalian cells, the autophagosomes produced in response to group A *Streptococcus* invasion are larger than those seen in starvation conditions (Nakagawa *et al.*, 2004). According to those data, where the signal is not saturated, the level of Atg8 induced by group A *Streptococcus* invasion is higher than that induced by starvation, suggesting that the regulation of autophagosome size achieved by controlling the amount of Atg8 may be a conserved mechanism.

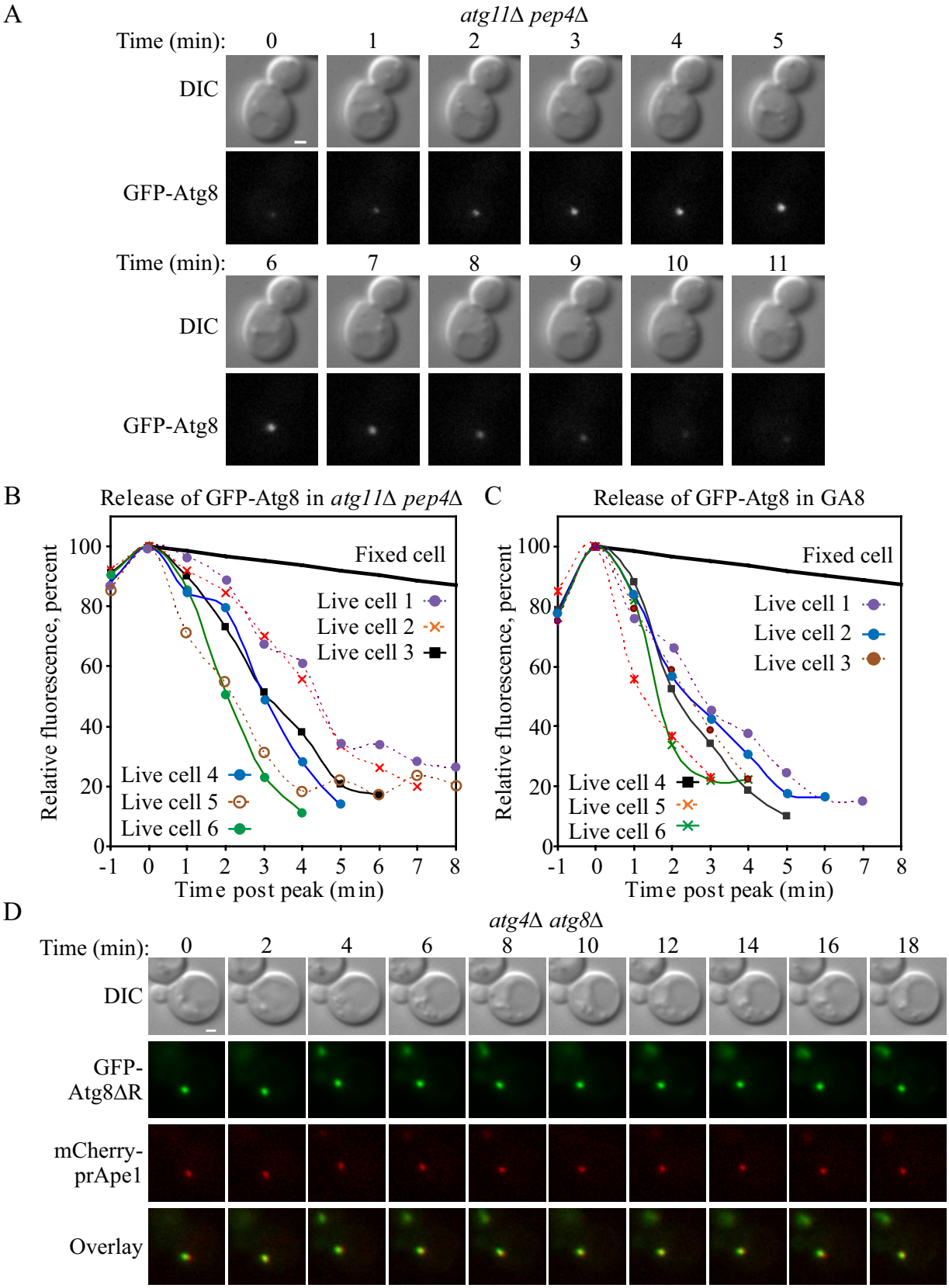

Figure 4. The majority of GFP-Atg8 at the PAS is released during autophagosome formation. (A) The decrease of signal intensity of GFP-Atg8 puncta is caused by the release of GFP-Atg8. GFP-Atg8 was expressed in *atg11*Δ *pep4*Δ cells. Yeast cells grown to midlog phase in nutrient-rich medium were collected and starved in nitrogen-starvation medium for 30 min. Microscopy observation was performed as in Figure 3. The signal decreases were evident in *atg11*Δ *pep4*Δ cells, which are defective in degradation of autophagic bodies. (B and C) The

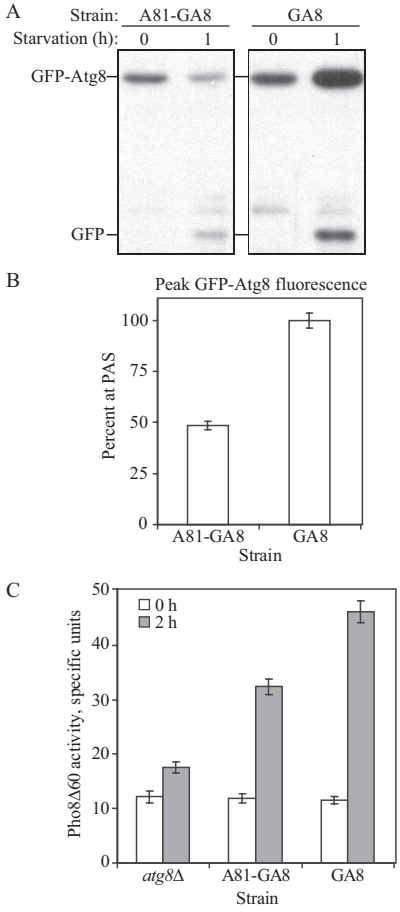

Figure 5. Amount of Atg8 at the PAS controls the level of autophagy. (A) Different amounts of GFP-Atg8 were expressed in strain A81-GA8 and GA8. GFP-Atg8 was expressed under the promoter used in strain A8-1 (strain A81-GA8) or its own promoter (strain GA8) in *atg8*Δ cells. Yeast cells were collected at the indicated time points after starvation. Protein extracts were analyzed by immunoblotting with anti-GFP antibody. GFP refers to the GFP moiety, which is stable in the vacuole, released as the result of GFP-Atg8 degradation. (B) The amount of Atg8 recruited to the PAS is limited by the protein level. Yeast cells were starved in nitrogen-starvation medium for 1 h. Microscopy observation was performed as in Figure 3. Average peak intensities during dynamic cycles are shown. The average peak intensity in strain GA8 is normalized as 100%. Error bar, SEM; $n > 100$. Lower amounts of GFP-Atg8 were recruited to the PAS in strain A81-GA8 compared with strain GA8. (C) The level of autophagy correlates with the amount of GFP-Atg8 recruited to the PAS. The Pho8Δ60 assay was performed as in Figure 1. Error bar, SEM from three independent repeats.

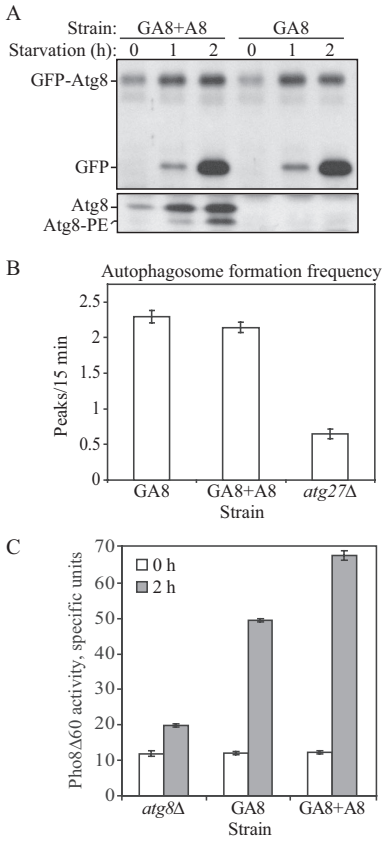

Figure 6. Atg8 does not control the frequency of autophagosome production. (A) GFP-Atg8 was expressed alone (strain GA8) or with additional Atg8 (strain GA8+A8). Samples were prepared as in Figure 5A. Protein extracts were analyzed by immunoblotting with anti-GFP antibody or anti-Atg8 antiserum. (B) Frequencies of autophagosome production in strains GA8 and GA8+A8 are comparable; the *atg27*Δ strain showed a significantly lower frequency. Yeast cells were starved for 1 h. The microscopy observation was performed as in Figure 3. The numbers of GFP-Atg8 peaks during 15 min were recorded. Error bar, SEM; $n > 100$. (C) Autophagy levels are different in strains GA8 and GA8+A8. The Pho8Δ60 assay was performed as in Figure 1. Error bar, SEM from three independent repeats.

Figure 4 (cont). significant decrease in fluorescence is not an artifact due to photobleaching. The intensities of GFP-Atg8 puncta in live cells and fixed cells were quantified. For live cells, the peak intensities were normalized as 100%, and the peaks were aligned to time 0. For fixed cells, the initial intensities were normalized as 100%. In fixed cells, photobleaching caused less than a 10% reduction in fluorescence after 5 min. In *atg11*Δ *pep4*Δ cells (B) and in strain GA8 (GFP-Atg8 in *atg8*Δ; C), the remaining fluorescence at the PAS was clearly below 50% at 5 min after peak. (D) Atg8 deconjugation is required for the release of Atg8 and completion of autophagosomes. GFP-Atg8ΔR and mCherry-prApe1 were expressed in *atg4*Δ *atg8*Δ cells. Yeast cells were starved for 1 h. Microscopy observation was performed as in Figure 3. GFP-Atg8 and mCherry-prApe1 persisted in a punctate structure during 20 min of observation. Scale bar, 1 μm.

For the first time, our data allowed temporal dissection of the autophagosome formation process based on real-time observations (Figures 3 and 4). Here we propose a five-stage model. In the first stage, cargos and factors required for the PAS recruitment of Atg8 arrive at the PAS; in stage 2, Atg8 arrives at the PAS and the Atg8-containing structure expands; stage 3 is a transitional step, allowing the completion of expansion and initiating release of Atg8 through deconjugation; in stage 4, additional Atg8 molecules are gradually released from the PAS; and in stage 5, the phagophore matures into an autophagosome, and some Atg8 molecules are trapped inside. Previously, the lack of a data-derived multistage model restricted most studies on autophagosome formation to the PAS recruitment-dependency of autophagy-related proteins. Our model provides the foundation for reanalysis of the functions of known autophagy-related proteins and for screening new genes whose products act at each stage. In addition, this model serves as a reference point to coordinate the dynamics of other autophagy-related genes. For instance, it would be interesting to find at which stage Atg9, a protein known to cycle between the PAS and

peripheral sites, departs from the PAS (Reggiori *et al.*, 2004; Young *et al.*, 2006).

Our results suggest that the expansion and deformation of the phagophore happens concurrently or slightly after the recruitment of Atg8 to the PAS, given that Atg8 is a causal factor in determination of autophagosome size. When Atg8 is released, the Atg8-containing structures retained their sizes (Figure S2), indicating that at this moment the expansion of the phagophore should be near completion, but not fully closed so that Atg8 molecules attached to the concave side of the phagophore (that will become the inner membrane of the autophagosome) can leave the membrane.

At present, how Atg8 modifies the phagophore to produce different-sized autophagosomes is not clear; however, our data indicate that Atg8 is essential in autophagosome formation. In rare cases (in ~1% of the cells), small vesicular structures can be observed in *atg8*Δ *pep4*Δ cells (Supplementary Figure S3). Previously, small autophagosome-like structures have also been detected in *atg8*Δ cells (Abeliovich *et al.*, 2000). Currently, the identity of these structures cannot be determined in the absence of an autophagic membrane marker other than Atg8. In addition, we note that similar rare structures can also be detected in *atg1*Δ *pep4*Δ *vps4*Δ cells, which are defective in autophagosome formation (Supplementary Figure S3). Further experiments are therefore needed to elucidate the nature of these vesicles.

ACKNOWLEDGMENTS

The authors thank Dr. Roger Tsien (University of California, San Diego) for providing the mCherry-URA3 plasmid. This work was supported by National Institutes of Health Public Health Service Grant GM53396 to D.J.K.

REFERENCES

Abeliovich, H., Dunn, W. A., Jr., Kim, J., and Klionsky, D. J. (2000). Dissection of autophagosome biogenesis into distinct nucleation and expansion steps. J. Cell Biol. *151*, 1025–1034.

Baba, M., Osumi, M., Scott, S. V., Klionsky, D. J., and Ohsumi, Y. (1997). Two distinct pathways for targeting proteins from the cytoplasm to the vacuole/lysosome. J. Cell Biol. *139*, 1687–1695.

Boland, B., and Nixon, R. A. (2006). Neuronal macroautophagy: from development to degeneration. Mol Aspects Med. *27*, 503–519.

Hanada, T., Noda, N. N., Satomi, Y., Ichimura, Y., Fujioka, Y., Takao, T., Inagaki, F., and Ohusmi, Y. (2007). The ATG12-ATG5 conjugate has a novel E3-like activity for protein lipidation in autophagy. J. Biol. Chem. 282, 37298–37302.

Hemelaar, J., Lelyveld, V. S., Kessler, B. M., and Ploegh, H. L. (2003). A single protease, Apg4B, is specific for the autophagy-related ubiquitin-like proteins GATE-16, MAP1-LC3, GABARAP, and Apg8L. J. Biol. Chem. *278*, 51841–51850.

Huang, W.-P., Scott, S. V., Kim, J., and Klionsky, D. J. (2000). The itinerary of a vesicle component, Aut7p/Cvt5p, terminates in the yeast vacuole via the autophagy/Cvt pathways. J. Biol. Chem. *275*, 5845–5851.

Ichimura, Y. *et al.* (2000). A ubiquitin-like system mediates protein lipidation. Nature *408*, 488–492.

Kabeya, Y., Mizushima, N., Ueno, T., Yamamoto, A., Kirisako, T., Noda, T., Kominami, E., Ohsumi, Y., and Yoshimori, T. (2000). LC3, a mammalian homologue of yeast Apg8p, is localized in autophagosome membranes after processing. EMBO J. *19*, 5720–5728.

Kabeya, Y., Mizushima, N., Yamamoto, A., Oshitani-Okamoto, S., Ohsumi, Y., and Yoshimori, T. (2004). LC3, GABARAP and GATE16 localize to autophagosomal membrane depending on form-II formation. J. Cell Sci. *117*, 2805–2812.

Kametaka, S., Okano, T., Ohsumi, M., and Ohsumi, Y. (1998). Apg14p and Apg6/Vps30p form a protein complex essential for autophagy in the yeast, *Saccharomyces cerevisiae*. J. Biol. Chem. *273*, 22284–22291.

Kim, J., Huang, W.-P., Stromhaug, P. E., and Klionsky, D. J. (2002). Convergence of multiple autophagy and cytoplasm to vacuole targeting components to a perivacuolar membrane compartment prior to *de novo* vesicle formation. J. Biol. Chem. *277*, 763–773.

Kim, J., Huang, W.-P., and Klionsky, D. J. (2001). Membrane recruitment of Aut7p in the autophagy and cytoplasm to vacuole targeting pathways requires Aut1p, Aut2p, and the autophagy conjugation complex. J. Cell Biol. *152*, 51–64.

Kirisako, T., Baba, M., Ishihara, N., Miyazawa, K., Ohsumi, M., Yoshimori, T., Noda, T., and Ohsumi, Y. (1999). Formation process of autophagosome is traced with Apg8/Aut7p in yeast. J. Cell Biol. *147*, 435–446.

Kirisako, T. *et al.* (2000). The reversible modification regulates the membrane-binding state of Apg8/Aut7 essential for autophagy and the cytoplasm to vacuole targeting pathway. J. Cell Biol. *151*, 263–276.

Klionsky, D. J., Cuervo, A. M., and Seglen, P. O. (2007). Methods for monitoring autophagy from yeast to human. Autophagy *3*, 181–206.

Kuma, A., Mizushima, N., Ishihara, N., and Ohsumi, Y. (2002). Formation of the approximately 350-kDa Apg12-Apg5·Apg16 multimeric complex, mediated by Apg16 oligomerization, is essential for autophagy in yeast. J. Biol. Chem. *277*, 18619–18625.

Levine, B., and Klionsky, D. J. (2004). Development by self-digestion: molecular mechanisms and biological functions of autophagy. Dev. Cell *6*, 463–477.

Mizushima, N., Kuma, A., Kobayashi, Y., Yamamoto, A., Matsubae, M., Takao, T., Natsume, T., Ohsumi, Y., and Yoshimori, T. (2003). Mouse Apg16L, a novel WD-repeat protein, targets to the autophagic isolation membrane with the Apg12-Apg5 conjugate. J. Cell Sci. *116*, 1679–1688.

Mizushima, N., Noda, T., Yoshimori, T., Tanaka, Y., Ishii, T., George, M. D., Klionsky, D. J., Ohsumi, M., and Ohsumi, Y. (1998a). A protein conjugation system essential for autophagy. Nature *395*, 395–398.

Mizushima, N., Sugita, H., Yoshimori, T., and Ohsumi, Y. (1998b). A new protein conjugation system in human. The counterpart of the yeast Apg12p conjugation system essential for autophagy. J. Biol. Chem. *273*, 33889–33892.

Nakagawa, I. *et al.* (2004). Autophagy defends cells against invading group A *Streptococcus*. Science *306*, 1037–1040.

Noda, T., Matsuura, A., Wada, Y., and Ohsumi, Y. (1995). Novel system for monitoring autophagy in the yeast *Saccharomyces cerevisiae*. Biochem. Biophys. Res. Commun. *210*, 126–132.

Paz, Y., Elazar, Z., and Fass, D. (2000). Structure of GATE-16, membrane transport modulator and mammalian ortholog of autophagocytosis factor Aut7p. J. Biol. Chem. *275*, 25445–25450.

Reggiori, F., Shintani, T., Nair, U., and Klionsky, D. J. (2005). Atg9 cycles between mitochondria and the pre-autophagosomal structure in yeasts. Autophagy *1*, 101–109.

Reggiori, F., Tucker, K. A., Stromhaug, P. E., and Klionsky, D. J. (2004). The Atg1-Atg13 complex regulates Atg9 and Atg23 retrieval transport from the pre-autophagosomal structure. Dev. Cell *6*, 79–90.

Schmid, D., and Münz, C. (2007). Innate and adaptive immunity through autophagy. Immunity *27*, 11–21.

Shaner, N. C., Campbell, R. E., Steinbach, P. A., Giepmans, B. N. G., Palmer, A. E., and Tsien, R. Y. (2004). Improved monomeric red, orange and yellow fluorescent proteins derived from *Discosoma* sp. red fluorescent protein. Nat. Biotechnol. *22*, 1567–1572.

Shintani, T., Huang, W.-P., Stromhaug, P. E., and Klionsky, D. J. (2002). Mechanism of cargo selection in the cytoplasm to vacuole targeting pathway. Dev. Cell. *3*, 825–837.

Shintani, T., and Klionsky, D. J. (2004a). Autophagy in health and disease: a double-edged sword. Science. *306*, 990–995.

Shintani, T., and Klionsky, D. J. (2004b). Cargo proteins facilitate the formation of transport vesicles in the cytoplasm to vacuole targeting pathway. J. Biol. Chem. *279*, 29889–29894.

Suzuki, K., Kirisako, T., Kamada, Y., Mizushima, N., Noda, T., and Ohsumi, Y. (2001). The pre-autophagosomal structure organized by concerted functions of *APG* genes is essential for autophagosome formation. EMBO J. *20*, 5971–5981.

Suzuki, K., Kubota, Y., Sekito, T., and Ohsumi, Y. (2007). Hierarchy of Atg proteins in pre-autophagosomal structure organization. Genes Cells. *12*, 209–218.

Tanida, I., Minematsu-Ikeguchi, N., Ueno, T., and Kominami, E. (2005). Lysosomal turnover, but not a cellular level, of endogenous LC3 is a marker for autophagy. Autophagy. *1*, 84–91.

Tanida, I., Mizushima, N., Kiyooka, M., Ohsumi, M., Ueno, T., Ohsumi, Y., and Kominami, E. (1999). Apg7p/Cvt2p: a novel protein-activating enzyme essential for autophagy. Mol. Biol. Cell *10*, 1367–1379.

Tanida, I., Tanida-Miyake, E., Komatsu, M., Ueno, T., and Kominami, E. (2002). Human Apg3p/Aut1p homologue is an authentic E2 enzyme for multiple substrates, GATE-16, GABARAP, and MAP-LC3, and facilitates the conjugation of hApg12p to hApg5p. J. Biol. Chem. *277*, 13739–13744.

Tanida, I., Tanida-Miyake, E., Ueno, T., and Kominami, E. (2001). The human homolog of *Saccharomyces cerevisiae* Apg7p is a protein-activating enzyme for multiple substrates including human Apg12p, GATE-16, GABARAP, and MAP-LC3. J. Biol. Chem. *276*, 1701–1706.

Tsukada, M., and Ohsumi, Y. (1993). Isolation and characterization of autophagy-defective mutants of *Saccharomyces cerevisiae*. FEBS Lett. *333*, 169–174.

Xie, Z., and Klionsky, D. J. (2007). Autophagosome formation: core machinery and adaptations. Nat. Cell Biol. *9*, 1102–1109.

Yen, W.-L., Legakis, J. E., Nair, U., and Klionsky, D. J. (2007). Atg27 is required for autophagy-dependent cycling of Atg9. Mol. Biol. Cell *18*, 581–593.

Yorimitsu, T., and Klionsky, D. J. (2005). Autophagy: molecular machinery for self-eating. Cell Death Differ. *12*, 1542–1552.

Young, A.R.J., Chan, E.Y.W., Hu, X. W., Köchl, R., Crawshaw, S. G., High, S., Hailey, D. W., Lippincott-Schwartz, J., and Tooze, S. A. (2006). Starvation and ULK1-dependent cycling of mammalian Atg9 between the TGN and endosomes. J. Cell Sci. *119*, 3888–3900.